J Fluoresc (2008) 18:1163–1168
DOI 10.1007/s10895-008-0368-4

ORIGINAL PAPER

Correlation Between Autofluorescence Intensity and Tumor Area in Mice Bearing Renal Cell Carcinoma

Maria Helena Bellini · Enia Lúcia Coutinho · Lilia Coronato Courrol · Flávia Rodrigues de Oliveira Silva · Nilson Dias Vieira Júnior · Nestor Schor

Received: 19 January 2008 / Accepted: 14 March 2008 / Published online: 17 May 2008

Abstract Protoporphyrin IX (PpIX) is a porphyrin derivative that is accumulated in cancerous tissue in consequence of the tumor-specific metabolic alterations. The aim of this study was to evaluate the accumulation of PpIX in mice bearing renal cell carcinoma by spectroscopy analysis. A total of 24 male Balb/c mice, 6 weeks old, were divided into six groups: Normal (without inoculation of tumor cells) and 4, 8, 13, 16, and 20 days after inoculation of tumor cells. The orthotopic tumor model of renal cancer was used. Murine renal cell carcinoma (Renca cells) were inoculated into the subcapsular space of the kidney. Normal and tumor-bearing kidneys in different progression stages were removed and analyzed by ex-vivo spectroscopy and by microscopy, for tumor histometric analysis. Emission spectra were obtained by exciting the samples at 405 nm. Significant differences between normal and tumor-bearing kidneys in autofluorescence shape occurred in the 600–700 nm spectral region. A good correlation was found between emission band intensity at 635 nm and the tumor area.

Keywords Renal carcinoma · Porphyrin · Fluorescence · Tumor growth

M. H. Bellini (✉) · E. L. Coutinho · N. Schor
Disciplina de Nefrologia, Departamento de Medicina, UNIFESP, São Paulo, SP, Brazil
e-mail: mhmarumo@terra.com.br

M. H. Bellini
Centro de Química e Meio Ambiente, IPEN/CNEN-SP, São Paulo, SP, Brazil

L. C. Courrol
Departamento de Ciências Químicas, Físicas e Matemáticas, UNIFESP, São Paulo, SP, Brazil

F. Rodrigues de Oliveira Silva
Departamento de Engenharia Elétrica, Escola Politécnica da USP, São Paulo, SP, Brazil

N. D. Vieira Júnior
Centro de Lasers e Aplicações, IPEN/CNEN-SP, São Paulo, SP, Brazil

Introduction

Renal cell carcinoma (RCC) is the eighth most common tumor in men and the 11th most common in women. During the past two decades, the incidence of renal cell carcinoma has increased by approximately 2% per year [1, 2]. In the USA, RCC represents the third leading cause of death among genitourinary malignancies, and the 12th leading cause of cancer death overall. Conventional chemotherapy is ineffective, since RCC cells overexpress genes that confer resistance to multiple drugs, and radiotherapy is only useful for palliation of tumor symptoms [3, 4]. Systemic immunotherapy protocols using IFN-α, interleukin-2, or a combination of both were designed. However, results of large clinical trials have shown overall poor objective responses (<20% of the patients were somehow responsive) and of short duration, accompanied with severe toxicities [5–7]. RCC secrete the proangiogenic cytokines vascular endothelial growth factor (VEGF) and platelet-derived growth factor (PDGF) in vitro and in vivo, which are responsible for the tumor-associated angiogenesis [8]. Altogether, these studies suggested that the vascularization in RCC might be an effective target for novel therapeutic approaches, as it has been proposed for a variety of tumor progression models [9]. Surgery remains

the only curative treatment for almost all renal tumors, especially RCC. Open radical nephrectomy, has long been the gold standard treatment for localized RCC. Nevertheless, as a consequence of increased detection of small tumors other potential therapeutic options arose in an attempt to minimize operative morbidity such as partial nephrectomy, cryoablation, radiofrequency ablation and high-intensity focused ultrasound [10, 11]. Early diagnosis and localization of RCC play an important role in its prevention and successful treatment. Kidney-preserving tumor resection is an alternative treatment for RCC <4 cm in diameter.

Native cellular fluorescence represents the innate capacity of tissues to absorb and emit light of specified wavelengths. Autofluorescence in living tissue is based on the presence of fluorophores such as elastin, collagen, tryptophan, flavins and porphyrins [12]. Protoporphyrin IX (PpIX) is a porphyrin derivative that is accumulated in cancerous tissue in consequence of the tumor-specific metabolic alterations. Several studies have been performed to define the potential of autofluorescence for cancer diagnosis [13–15]. The advantage of using exogenous fluorophores is that the photophysical and pharmacokinetic properties can be selected and are known [16].

PpIX is a porphyrin derivative that combines with ferrous iron to form the heme of hemoglobin and with ferric or ferrous iron to form the prosthetic groups of substances, such as myoglobin, catalase, and the cytochromes. Abnormal PpIX metabolism has been observed in the blood, plasma, serum and other tissues of cancer patients, indicating that cancer cells accumulate substantially more PpIX than the normal cells and tissues [17–20]. The enhanced fluorescence of endogenous porphyrins in cancerous tissues is assumed to be a consequence of the tumor-specific metabolic alterations which can be caused by tumor hypervascularity [13–15, 20]. When PpIX is irradiated at wavelengths from 390 to 440 nm, it fluoresces at 635 nm (red) and can be used to identify tumor cells. In addition, selective accumulation of the PpIX in tumors and in precancerous lesions can be increased by the use of exogenous substances, particularly 5-aminolevulinic acid (ALA). The use of ALA has been investigated for detection and therapy of tumors in a number of organs, such as the skin, the bladder and the gastrointestinal [21].

The fluorescence spectroscopy technique appears to be very important in cancer diagnosis. Fluorescence detection has advantages over other light-based investigation methods: high sensitivity, high speed, safety, and the possibility of being used for real-time diagnosis.

The aim of this study was to examine the accumulation of PpIX in normal and tumor-bearing kidneys in different progression stages by ex-vivo spectroscopy and by microscopy.

Materials and methods

Cell line and cell culture conditions

Murine renal cell carcinoma (Renca cells) was kindly donated by Dr. Isaiah J. Fidler (The University of Texas M. D. Anderson Cancer Center, Houston, TX) and were cultured in RPMI with a high glucose content (4.5 g/L at 25 mM) and supplemented with 100 U/ml penicillin, 50 mg/ml streptomycin, and 10% FBS. The cells were maintained in a humid chamber at 37 °C and 5% CO_2.

Animals and tumor induction

A total of 24 male Balb/c mice, ~6 weeks old on arrival, were obtained from INFAR UNIFESP-EPM. The mice were divided into six groups: one normal (without inoculation of tumor cells) and five tumor-cell-bearing groups killed after 4, 8, 13, 16, and 20 days from tumor cell inoculation, respectively. The orthotopic tumor model of renal cancer was used. Renca cells were inoculated (1×10^5 cells/animal) into the subcapsular space of the kidney with a 30-G needle, in a volume of 0.1 mL sterile phosphate-buffered saline (PBS).

Tumor excision and histological analysis

The animals used in the experiments were sacrificed following the guidelines for euthanasia of the American Veterinarian Medical Association. On a specific day of the bioassay, the animals were sacrificed and the kidneys were excised. Half of each kidney was washed in PBS, fixed in 10% PBS-buffered formalin for 24 h, and then routinely processed for paraffin-embedding. The other half was washed in sterile PBS and then cryopreserved in dry ice until spectroscopy analysis. Histological analysis was performed in 4 μm sections stained with hematoxylin and

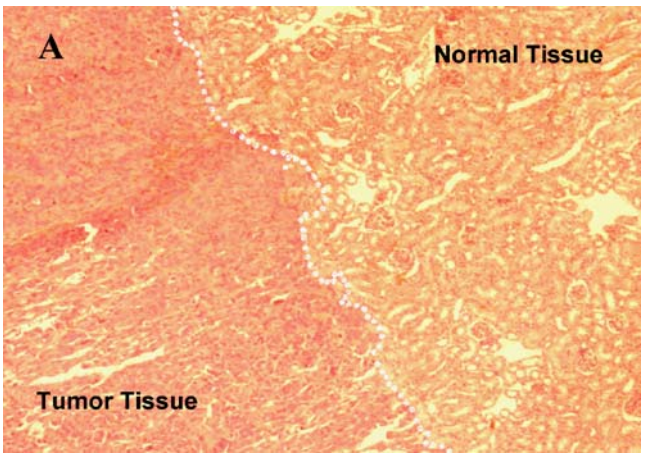

Fig. 1 Histological slide of 8-days tumor-cell inoculated kidney. Definition of the border between RCC and surrounding healthy tissue

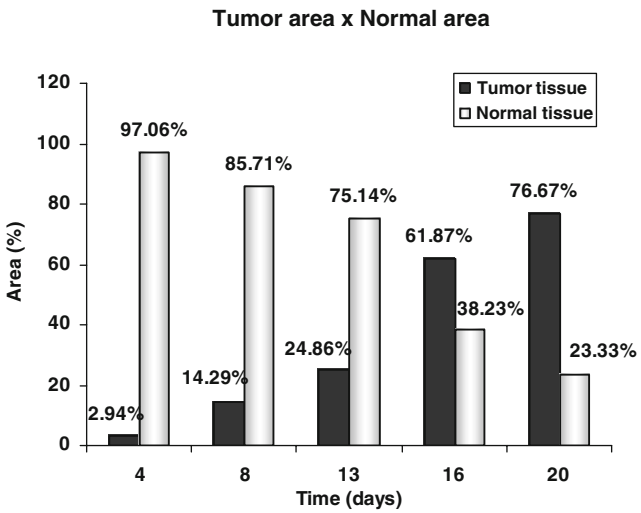

Fig. 2 Histological analyses of tumor and normal kidney areas after 4, 8, 13, 16, and 20 days from orthotopic Renca cells inoculation

eosin. The tumor area was quantified as follows: grids were projected on random fields of tumor sections at a 20× magnification, and the number of grid intersections overlaying stained tumor cells was counted. Twenty fields were counted per tumor. Data were expressed as the relative area of tumor cells within the tumor parenchyma.

Fluorescent spectral analysis

After surgery, the kidneys were conserved in dry ice. The normal and inoculated kidneys were measured after few hours of extraction. The tissue autofluorescence was measured perpendicularly, with excitation at 405 nm obtained with a 150 W Xenon lamp beam and a 0.25 m Jarrel Ash monochromator. The excitation light was focused in the sample with a 10 cm lens. For the comparisons between different samples, we always used the same sample geometry and light intensity. The emissions of the samples were analyzed with a 0.5 m Spex monochromator and a PMT detector in a home made configuration. The signal was amplified with an EG&G 7220 lock-in amplifier and processed by computer.

Statistical analysis

Statistical analysis of the differences between the experimental groups was performed by applying Student's t test. Significance was set at $P<0.05$. Data are expressed as mean±SE.

Results

Histological analysis of the tumor

Histological analysis of all the samples used in this tumor progression study evidenced proliferating tumor cell areas. These areas were used for spectroscopy analysis. Figure 1 shows the microscopy definition of the border between the RCC and the surrounding healthy tissue.

Analyses of tumor-bearing kidneys were performed at all points of the experiments, to evaluate the tumor progression

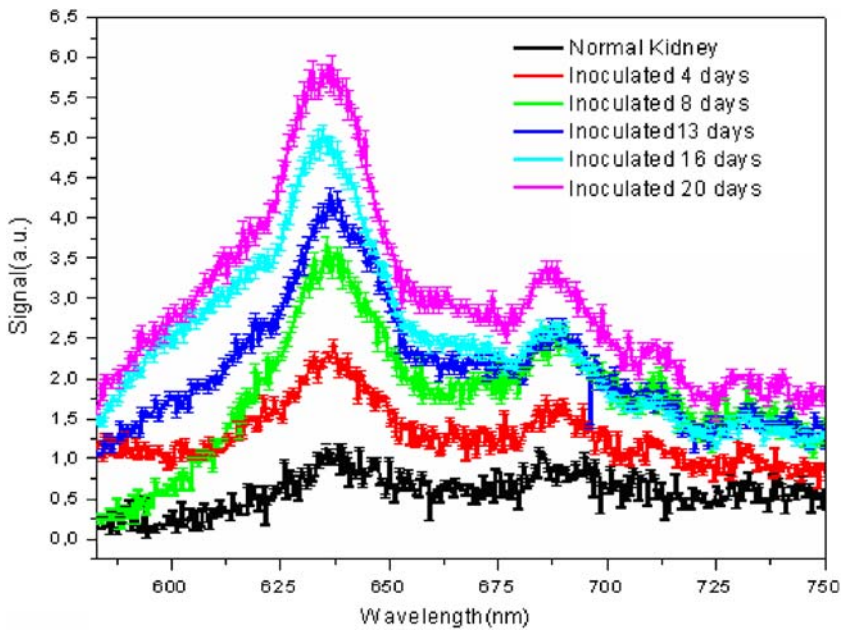

Fig. 3 Mean autofluorescence spectra of healthy and tumor-cell-bearing kidneys after 4, 8, 13, 16, and 20 days from orthotopically implanted Renca cells. The values are the mean and SE of three healthy kidneys and three inoculated kidneys from each group

Table 1 Tumor area and fluorescence intensity (~635 nm) for normal and tumor-bearing kidneys after 4, 8, 13, 16, and 20 days from orthotopic Renca cell inoculation

	Tumor area (%)	Fluorescence intensity (a.u.[a])	Standard error
Normal	–	0.80	0.048
4 days	2.94	2.40	0.037
8 days	14.29	3.54	0.020
13 days	24.86	4.21	0.024
16 days	61.87	4.98	0.038
20 days	76.67	5.80	0.035

Emission intensity of normal kidneys was significantly different from tumor-bearing kidneys ($p<0.05$ for all comparisons, Student's t test).
[a] Arbitrary unit

and to investigate a possible correlation between tumor mass growth and fluorescence emission. Analysis of tumor cells in situ, using HE staining, indicated a linear increase of the tumor area during the experiment. Quantitative analysis of these sections showed that within 4 days from inoculation the tumor mass had reached 2.94% of the kidney area and that the emission intensity of this tumor was twice that of a normal kidney. This result shows how sensitive this method is (Fig. 2).

Autofluorescence study

Ex-vivo autofluorescence spectra were recorded for 20 tumor tissue and four healthy kidney specimens, and the fluorescence spectra at 583–750 nm were analyzed. The fluorescence spectra of normal and tumor tissues in different stages of progression are presented in Fig. 3. The significant differences between normal and tumor tissue in autofluorescence shape occurred in the 600–700 nm spectral region. The spectrum consists of three main peaks around 600, 635 and 690 nm, which are typical for free protoporphyrin IX. In fact, a most intense fluorescence peak was observed at ~635 nm. The intensity behavior showed a very good correlation with tumor area.

Table 1 shows the tumor areas (%) and fluorescence intensity at ~635 nm, as shown by spectroscopy analysis. The increase in fluorescence accompanied the growth of the tumor mass was at all points significantly different from the values obtained for the normal kidneys. These findings demonstrate a true endogenous accumulation of PpIX by RCC cells, probably caused by tumor-specific metabolic alterations and renal tumor hypervascularity.

Tumor and spectral profile analysis

A panel of histological slides (a, b, c) and the corresponding emission spectra (d, e, f) of normal and inoculated kidneys (8, 20 days) are shown in Fig. 4. The normal kidney samples did not show any characteristic fluorescence band (a, d). On the other hand, it was clear that the increase in peak fluorescence at ~635 nm in the inoculated kidneys was positively correlated with tumor stage progression (b, e; c, f)

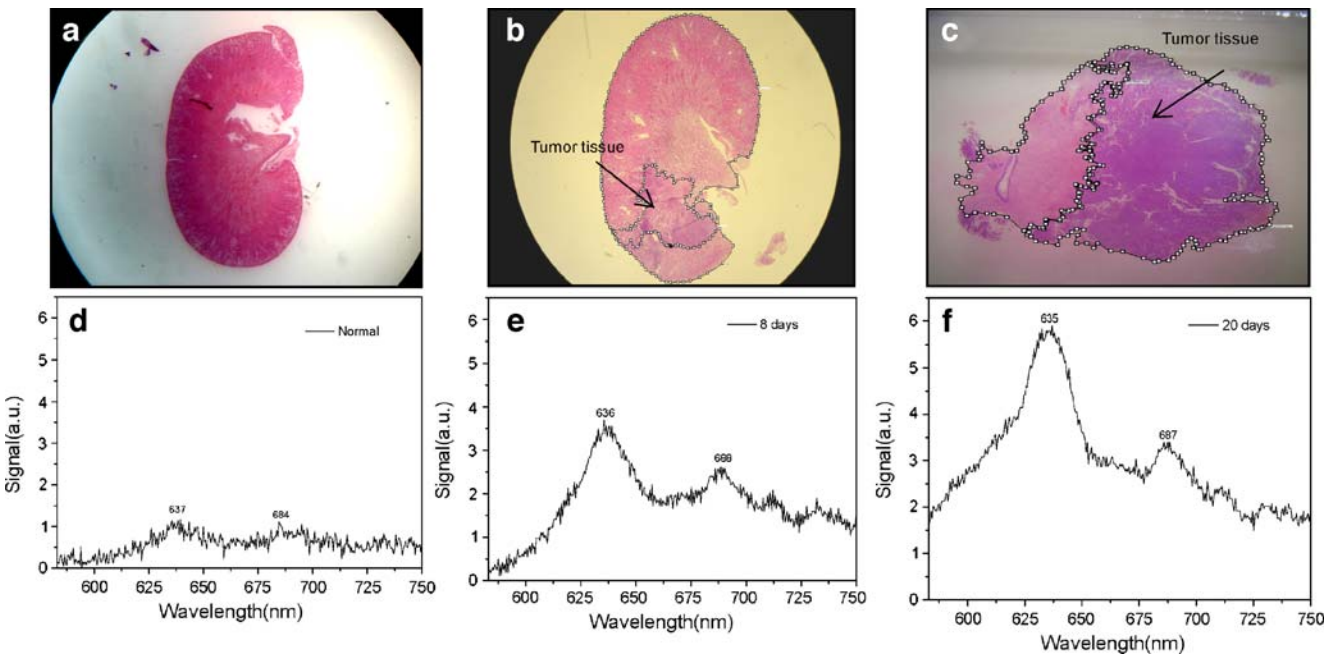

Fig. 4 Correlation between tumor area and peak fluorescence at 635 nm in normal (**a**, **d**) and tumor-inoculated kidneys (**b**, **e**=8 days; **c**, **f**=20 days)

Discussion

Optical spectroscopy can measure changes in tissue by quantifying differences in a tissue's spectral properties—its ability to absorb, emit, and scatter light at various wavelengths. Animal tissue autofluorescence is caused by endogenous fluorophores, including elastin and collagen (400 nm), tryptophan (350 nm), flavins (520–540 nm) and porphyrins (600–700 nm) [22]. The autofluorescence of individual components can be used to contrast different types of biological tissue or cellular metabolism. Malignant cells commonly display altered metabolism, and this characteristic can be used to attack or diagnose them. The endogenous fluorophores that are speculated to cancerous transformations are the amino acids tryptophan and tyrosine, the structural proteins collagen and elastin, the coenzymes NAD(P)H and FAD, and phorphyrins [22]. Several studies have been performed to define the potential of autofluorescence for cancer diagnosis and therapy [23, 24].

RCC is the most frequently occurring malignant tumor of the renal parenchyma. For small tumors, conservative resection have been considered an alternative treatment and after this procedure, the 5-year survival is estimated to be 80–100% and the rate of local recurrence as being <10% [25, 26].

In the present study, a murine model of tumor progression was used. After implantation of RCC into mice kidneys, intrarenal tumors were formed, with a clear macroscopic and microscopic definition of the border between the RCC and the surrounding healthy tissue.

Our results indicate that the fluorescence spectra of all cancer tissue samples exhibited main peaks: at ~635 and ~689 nm. These peaks, showed in red, are characteristic for PpIX [21]. They were also identified in plasma and tumors from mice bearing hepatoma [19, 20]. We observed a major difference in emission band intensity at 635 nm, and photodetection of RCC was possible after only 4 days from inoculation, when the tumor amounted to no more than 2.94% of the kidney area. In fact, this method is very sensitive as the emission band at 635 nm of small tumor masses showed the double of the intensity compared to the normal tissue. Besides, the sensitivity of this method is very high.

A good correlation was found between emission band intensity at 635 nm and the size of the tumor area. It is clear that fluorescence intensity increases with the growth of the tumor mass. Considering that the fluorescence detected in the tumors was due to the presence of endogenous PpIX, we suggest that in RCC the metabolism is affected ever since the early stages of tumor development and this optical spectroscopy technique is quantitative.

In a previous study [13], our group has demonstrated the autofluorescence of blood PpIX in xenoimplanted SCID mice and an increase in fluorescence intensity at ~635 nm as a function of growth of subcutaneous tumor mass. Taken together, these results indicate that fluorescence spectroscopy of PpIX may be a useful tool in the diagnosis and therapy of RCC.

Conclusions

In conclusion, the fluorescence and excitation techniques appear quite useful for detect tumor mass, even the small ones.

This technique may be helpful in defining resection limits when planning conservative kidney-preserving surgery for RCC. Besides, it might enrich the surgeon's armamentarium and can be used in favor to minimally invasive therapies.

Acknowledgements This study was supported by FAPESP (process number: 03/11779-9).The expert assistance of Rodolfo Nürmberg Junior, Ph.D., was highly appreciated.

References

1. Lipwortha L, Taronea RE, McLaughlina JK (2006) The epidemiology of renal cell carcinoma. Review article. J Urol 176(6):2353–2358
2. Thomas E, Hutson DO (2005) Renal cell carcinoma: diagnosis and treatment, 1994–2003. Proc Bayl Univ Med Cent 18(4):337–340
3. Mignogna C, Staibano S, Altieri V, De Rosa G, Pannone G, Santoro A, Zamparese R, D'Armiento M, Rocchetti R, Mezza E, Nasti M, Strazzullo V, Montanaro V, Mascolo M, Bufo P (2006) Prognostic significance of multidrug-resistance protein (MDR-1) in renal clear cell carcinomas: a five year follow-up analysis. BMC Cancer 19(6):293
4. Lebret T (2007) What is the role of adjuvant therapy after nephrectomy? (Review article). Prog Urol 17(1 Suppl 1):148–149
5. Hudes G, Carducci M, Tomczak P, Dutcher J, Figlin R, Kapoor A, Staroslawska E, Sosman J, McDermott D, Bodrogi I, Kovacevic Z, Lesovoy V, Schmidt-Wolf IG, Barbarash O, Gokmen E, O'Toole T, Lustgarten S, Moore L, Motzer RJ (2007) Temsirolimus, interferon alfa, or both for advanced renal-cell carcinoma. Global ARCC Trial. N Engl J Med 356(22):2271–2281
6. Hutson TE (2007) Targeted therapy for renal cell carcinoma: a new treatment paradigm. Proc Bayl Univ Med Cent 20(3):244–248
7. Escudier B (2007) Advanced renal cell carcinoma: current and emerging management strategies. Drugs 67(9):1257–1264
8. Jacobson J, Rasmuson T, Grankvist K, Ljungberg B (2000) Vascular endothelial growth factor as prognostic factor in renal cell carcinoma. J Urol 163:343–347
9. Coutinho EL, Chammas R, Morganti L, Schor N, Bellini MH (2007) Anti-tumor effect of endostatin mediated by retroviral gene transfer in mice bearing renal cell carcinoma. Faseb J 21 (12):3153–3161
10. Eeckt VK, Joniau S, Van Poppel H (2007) Open surgery for localized RCC. Sci World J 7:742–752

11. Rodríguez-Covarrubias F, Gabilondo B, Borgen JL, Gabilondo F (2007) Partial nephrectomy for renal tumors using selective parenchymal clamping. Int Urol Nephrol 39:43–46
12. Schantz SP, Savage HE, Sacks P, Alfano RR (1997) Native cellular fluorescence and its application to cancer prevention. Environ Health Perspect 105(Suppl 4):941–944
13. Van Der Breggen EWJ, Rem AI, Cristian MM, Yang CJ, Calhoun KH, Sterenborg HJCM, Motamedi M (1996) Spectroscopic detection of oral and skin tissue transformation in a model for squamous cell carcinoma: autofluorescence versus systemic aminolevulinic acid-induced fluorescence. IEEE J Sel Top Quantum Electron 2:997–1007
14. Moesta KT, Ebert B, Handke T, Nolte D, Nowak C, Haensch WE, Pandey RK, Dougherty TJ, Rinneberg H, Schlag PM (2001) Protoporphyrin IX occurs naturally in colorectal cancers and their metastases. Cancer Res 61:991–999
15. Courrol LC, Silva FRO, Coutinho EL, Piccoli MF, Mansano RD, Vieira ND, Schor N, Bellini MH (2007) Study of blood porphyrin spectral profile for diagnosis of tumor progression. J Fluoresc 17 (3):289–292
16. Ramanujan N (2000) Fluorescence spectroscopy of neoplastic and non-neoplastic tissues. Neoplasia 2(1–2):89–117
17. Kusunoki Y, Imamura F, Uda H, Mano M, Horai T (2000) Early detection of lung cancer with laser-induced fluorescence endoscopy and spectrofluorometry. Chest 118:1776–1782
18. Tsai TM, Hong RL, Tsai JC et al (2004) Effect of 5-aminolevulinic acid-mediated photodynamic therapy on MCF-7 and MCF-7/ADR cells. Lasers Surg Med 34:64–72
19. Heyerdahl H, Wang I, Liu DL, Berg R, Andersson-Engels S, Peng Q, Moan J, Svanberg S, Svanberg K (1997) Pharmacokinetic studies on 5-aminolevulinic acid-induced protoporphyrin IX, accumulation in tumors and normal tissues. Cancer Lett 112:225–231
20. Malik Z, Kostenich G, Roitman L, Ehrenberg B, Orenstein A (1995) Topical application of 5-aminolevulinic acid, DMSO and EDTA: protoporphyrin IX accumulation in skin and tumors of mice. J Photochem Photobiol B Biol 28:213–218
21. Triesscheijn M, Baas P, Schellens JHM, Stewart FA (2006) Photodynamic therapy in oncology. Oncologist 11(9):1034–1044
22. Ramanujam N (2000) Fluorescence spectroscopy of neoplastic and non-neoplastic tissues. Neoplasia 2(1–2):89–117
23. Tamosiunas M, Makaryceva J, Labanauskiene J, Bagdonas S, Aleksandraviciene C, Didziapetriene J, Griciute L, Rotomskis R (2004) Autofluorescence of transplantable hepatoma a22 [mh-a22]: prospects of tumor tissue optical biopsy. Exp Oncol 26 (2):118–124
24. Meng WJ, Wang JX, Ma PH, Ren GX, Xu RX, Ren MW (1999) Protoporphyrin IX fluorescence from the plasma of tumor-implanted mouse. J Lumin 84:251–254
25. Popken G, Wetterauer U, Schultze-Seemann W (1999) Kidney-preserving tumour resection in renal cell carcinoma with photodynamic detection by 5-aminolaevulinic acid: preclinical and preliminary clinical results. BJU Int 83(6):578–582
26. Russo P, Goetzl M, Simmons R, Katz J, Motzer R, Reuter V (2002) Partial nephrectomy: the rationale for expanding the indications. Ann Surg Oncol 9:680–687